

Raman-active phonons in $\text{Bi}_2\text{Sr}_{2-x}\text{La}_x\text{CuO}_{6+d}$: Phonon assignment and charge-redistribution effects

Minoru Osada and Masato Kakihana*

Materials and Structures Laboratory, Tokyo Institute of Technology, Nagatsuta 4259, Midori-ku, Yokohama 226, Japan

Mikael Käll and Lars Börjesson

Department of Applied Physics, Chalmers University of Technology, S41296 Göteborg, Sweden

Atsuyoshi Inoue and Masatomo Yashima

Materials and Structures Laboratory, Tokyo Institute of Technology, Nagatsuta 4259, Midori-ku, Yokohama 226, Japan

(Received 7 October 1996)

Phonon Raman spectra of $\text{Bi}_2\text{Sr}_{2-x}\text{La}_x\text{CuO}_{6+d}$ single crystals with x values close to 0, 0.4, and 0.8 have been investigated. Room-temperature measurements were performed in the five main polarization geometries, including the c -axis polarized configuration. We identify the $4A_{1g}$ symmetry modes that are Raman allowed within the ideal body-centered-tetragonal unit cell, as well as several disorder activated phonon bands from the BiO and/or SrO layers. For an increasing degree of La doping, the $O(2)_{\text{Sr}} A_{1g}$ mode at 624 cm^{-1} softens by 12 cm^{-1} between $x=0$ and $x=0.8$. We attribute this softening to a weakening of the $\text{Cu-O}(2)_{\text{Sr}}\text{-Bi}$ bond due to a reduction in Cu and Bi valences when going from the overdoped ($x=0$) to the underdoped ($x=0.8$) regime. [S0163-1829(97)04829-7]

I. INTRODUCTION

Since the discovery of high- T_c superconductivity in cuprates, Raman scattering has been extensively used in investigations of phonons and other low-energy excitations.¹ As opposed to the case of, e.g., $\text{YBa}_2\text{Cu}_3\text{O}_{7-d}$, the assignments of phonon eigenmodes in Raman spectra of the Bi-based high- T_c cuprates are still controversial.² For instance, the assignments of the two most prominent high-frequency oxygen modes at about 460 and 630 cm^{-1} in $\text{Bi}_2\text{Sr}_2\text{CaCu}_2\text{O}_{8+d}$ (Bi2212) and $\text{Bi}_2\text{Sr}_2\text{CuO}_{6+d}$ (Bi2201) have been much debated. The uncertainty in the phonon assignments can be traced to two facts. First, the complicated local structure of the BiO layers, characterized by an incommensurate superstructure^{3,4} as well as local atomic displacements,⁵ gives rise to a number of disorder-activated phonons, which complicates spectral interpretation. Secondary, the mica-like nature of Bi2212 and Bi2201 single crystals makes c -axis polarized measurements experimentally demanding, even though this scattering configuration has provided important phonon information in other high- T_c cuprates.

In a recent publication we argued that Raman measurements in the c -axis polarized geometry of $\text{Bi}_2\text{Sr}_2\text{Ca}_{1-x}\text{Y}_x\text{Cu}_2\text{O}_{8+d}$ (Ref. 2) were crucial for a correct phonon assignment. The two oxygen modes at ~ 460 and $\sim 630 \text{ cm}^{-1}$, for example, exhibit completely different polarization dependencies, which indicates that these two modes are connected with O_{Bi} and O_{Sr} vibrations along the c axis, respectively. In this paper we report Raman measurements on Bi2201 single crystals in the five main scattering geometries, i.e., including the important c -axis polarized configuration.

Another aspect considered in this work is the ‘‘charge-

redistribution’’ effect associated with the aliovalent substitution of La^{3+} for Sr^{2+} . It is now well established that La substitution continuously pushes the Bi2201 system from the heavily overdoped to the heavily underdoped regime, with a maximum T_c of $\approx 20 \text{ K}$ around $x \approx 0.4$.^{4,6,7} Here we report the hole-concentration dependence of phonon Raman spectra of $\text{Bi}_2\text{Sr}_{2-x}\text{La}_x\text{CuO}_{6+d}$ using three single crystals with x close to 0, 0.4, and 0.8 grown from melts doped with La. These La concentrations correspond to the overdoped, optimally doped, and underdoped regimes, respectively. Polycrystalline Raman spectra of $\text{Bi}_2\text{Sr}_{2-x}\text{La}_x\text{CuO}_{6+d}$ have been previously reported.^{8,9}

II. EXPERIMENT

Single crystals of $\text{Bi}_2\text{Sr}_{2-x}\text{La}_x\text{CuO}_{6+d}$ with x values close to 0, 0.4, and 0.8 were grown from the stoichiometric melts, as described in a separate publication.¹⁰ Typical dimensions were $\sim 5 \times 3 \times 0.1 \text{ mm}^3$. X-ray-diffraction measurements showed that the crystals were of the proper 2201 phase. The lattice parameter c was found to decrease with increasing La concentration: c being 24.698 , 24.391 , and 24.101 \AA for $x=0$, 0.4 , and 0.8 , respectively. Complex magnetic susceptibility measurements^{10,11} showed that the $x=0$ and $x=0.4$ samples were superconducting with critical transition temperatures of $T_c=7$ and 17 K , respectively, while the $x=0.8$ sample was nonsuperconducting down to 3 K .

Room-temperature Raman measurements were performed using freshly cleaved crystal surfaces. The laser beam ($\lambda = 514.5 \text{ nm}$) was focused to a $\sim 3 \mu\text{m}$ diameter spot by a $90\times$ microscope objective. The scattered light was analyzed with Jobin Yvon/Atago Bussan T64000 triple spectrometer and collected with a liquid-nitrogen-cooled CCD detector for $1500\text{--}3600 \text{ s}$. The spectral resolution was $2\text{--}3 \text{ cm}^{-1}$. Throughout this paper, the scattering configuration is defined

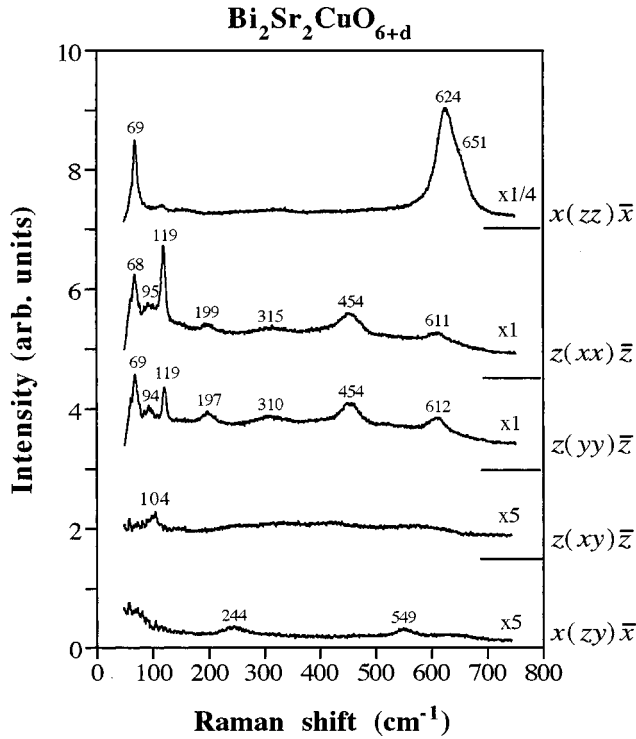


FIG. 1. Raman spectra of a $\text{Bi}_2\text{Sr}_2\text{CuO}_{6+d}$ single crystal in different scattering configurations. The short lines denote the zero-intensity level for the spectrum immediately above. Note the different intensity factors. Some of the lines below 150 cm^{-1} are due to rotational lines of air.

by notations such as $z(xx)\bar{z}$ (or xx , in short), which means that the incident light polarized along the x axis propagates along the z axis, and the scattered light polarized along the x axis propagates along the opposite z axis (i.e., \bar{z}). The coordinates (x, y, z) are chosen to coincide with the crystallographic axes (a, b, c) .

III. RESULTS AND DISCUSSION

A. Phonon Raman spectra of $\text{Bi}_2\text{Sr}_{2-x}\text{La}_x\text{CuO}_{6+d}$

Figure 1 shows typical Raman spectra of a $\text{Bi}_2\text{Sr}_2\text{CuO}_{6+d}$ single crystal at room temperature under the five main scattering configurations in the $50\text{--}745\text{ cm}^{-1}$ range. A group-theoretical analysis of a body-centered tetragonal unit cell of Bi2201 (space group $I4/mmm$) gives $4A_{1g}$ and $4E_g$ Raman-active vibrations,¹² with displacement vectors along the c and a axes, respectively. Note that only the BiO and SrO layers [i.e., the Sr , Bi , $\text{O}(2)_{\text{Sr}}$, and $\text{O}(3)_{\text{Bi}}$ ions] contribute to these even symmetry modes.

The Bi2201 xx and yy spectra of Fig. 1 exhibit two sharp low-frequency A_{1g} symmetry modes: the Bi vibration at $\sim 69\text{ cm}^{-1}$ and the Sr vibration at $\sim 119\text{ cm}^{-1}$. The zz spectrum exhibits, in addition to the Bi mode, an intense oxygen band at $\sim 624\text{ cm}^{-1}$. A comparison with Raman spectra of the Bi2212 (Ref. 2) and Bi1212 (Ref. 13) compounds gives strong evidence for assigning this phonon to the $\text{O}(2)_{\text{Sr}} A_{1g}$ mode, since both these structures exhibit intense zz polarized oxygen modes around $\sim 624\text{ cm}^{-1}$ and the only Raman-active oxygen ion common to all three structures is the $\text{O}(2)_{\text{Sr}}$. This assignment then implies that the exclusively

xx/yy polarized oxygen phonon at $\sim 454\text{ cm}^{-1}$ is due to the $\text{O}(3)_{\text{Bi}} A_{1g}$ mode. Note that the very different polarization dependencies of the 454- and 620-cm^{-1} phonons indicate that the $\text{O}(3)_{\text{Bi}}$ and $\text{O}(2)_{\text{Sr}}$ modes are largely decoupled, in contrast to the mixed character predicted from shell-model calculations.^{14,15} Since the assignments of the two high-frequency oxygen phonons have been much debated, we refer the interested reader to Ref. 2 for a thorough discussion of this topic. The depolarized zy spectrum of Fig. 1 exhibits two broad and weak bands around ~ 244 and $\sim 549\text{ cm}^{-1}$ probably induced by E_g -symmetry phonons. Figure 2 shows that polarization dependencies of each phonon are left more or less unchanged by the La substitution. This is also the case for the relative phonon intensities in each scattering configuration. All in all, the phonon frequencies and polarization dependencies in Figs. 1 and 2 are very similar to what has been observed in Bi2212 .²

In addition to the Raman-allowed phonons discussed above the spectra in Figs. 1 and 2 exhibit broad peaks around $95, 199, 315,$ and 651 cm^{-1} . The activation of these ‘‘extra’’ phonons is connected to the strongly distorted and nonideal structure of Bi2201 .^{3–5} Such modes are a common property of the Bi cuprates, in contrast to the case of the Tl cuprates (e.g., the Tl2201 compound¹⁶ isostructural to Bi2201). Since it is not clear which space group best describes the distorted crystal structure, group-theoretical analyses based on lower symmetry space groups would at best produce tentative assignments. In general we expect that these disorder-activated modes involve ion displacements within the BiO and/or SrO planes. It is known, for example, that the Bi and Sr atoms in Bi2201 exhibit large a -direction shifts from the ideal tetragonal sites compared to Cu .⁴ Also, the disorder-activated modes do not gain intensity with decreasing carrier concentration [i.e., with increasing La concentration; see, for instance, Figs. 2(a) and 2(b)] as is the case for CuO_2 -plane-derived phonons in, e.g., $\text{Bi}_2\text{Sr}_2\text{Ca}_{1-x}\text{Y}_x\text{Cu}_2\text{O}_{8+d}$.² It is possible that at least some of the disorder-related phonons in Bi2201 are activated by the well-known incommensurate superstructure formation through Brillouin-zone folding.¹⁷ In this respect, it is interesting that the shoulder of the $\text{O}(2)_{\text{Sr}}$ phonon, appearing at $\sim 651\text{ cm}^{-1}$ for the $x=0$ sample, becomes sharper and better resolved for increasing La doping [see Fig. 2(c)].¹⁸ This effect could be related to the incommensurate-to-commensurate superstructure transition that has been observed at around $x=0.8$ for La -doped Bi2201 ,³ as this would tend to decrease the disorder related width of a phonon activated through Brillouin-zone folding. Indeed, the band shape of this phonon mode appears to be very sensitive to the presence or absence of the modulation. For instance, the side band at higher frequencies disappears in the Raman spectra of modulation-free $\text{Bi}_{2-x}\text{Pb}_x\text{Sr}_2\text{CuO}_{6+d}$,^{8,19,20} where the $\text{Bi-O}(2)_{\text{Sr}}$ bonds should be vertically aligned in a more ordered way.

B. Charge-redistribution effects and apical-oxygen $\text{O}(2)_{\text{Sr}}$ phonon

The most prominent change in the phonon spectrum upon La substitution concerns the position of the $\text{O}(2)_{\text{Sr}}$ mode around $\sim 624\text{ cm}^{-1}$. This phonon softens by $\sim 12\text{ cm}^{-1}$ be-

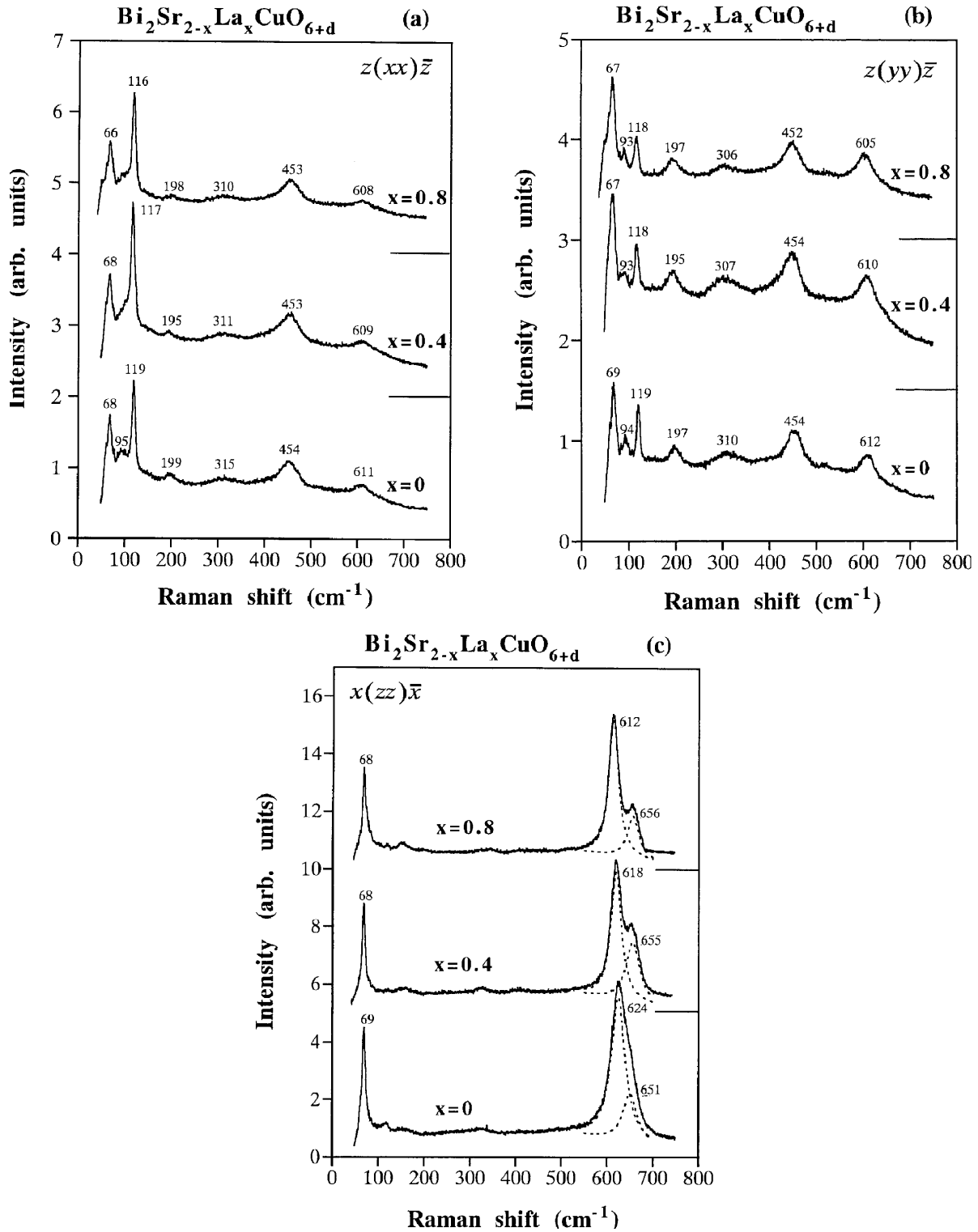


FIG. 2. Polarized micro-Raman spectra of $\text{Bi}_2\text{Sr}_{2-x}\text{La}_x\text{CuO}_{6+d}$ single crystals with $x=0, 0.4$, and 0.8 at room temperature in scattering configurations (a) $z(xx)\bar{z}$, (b) $z(yy)\bar{z}$, and (c) $x(zz)\bar{x}$. In (c) the dashed lines show the two-Lorentzian fits of partly overlapping A_{1g} bands in the high-frequency region ($550\text{--}700\text{ cm}^{-1}$) (Ref. 18). The short lines denote the zero-intensity level for the spectrum immediately above.

tween $x=0$ and 0.8 , as is clearly seen in the spectra of Fig. 2(c). From a structural point of view this is unexpected: the decrease in the average Sr/La ionic radius ($r_{\text{Sr}^{2+}}=1.26\text{ \AA}$, $r_{\text{La}^{3+}}=1.16\text{ \AA}$) for increasing x , which is reflected in a c -axis contraction by $\sim 2.5\%$ between $x=0$ and 0.8 (see above), should push the $\text{O}(2)_{\text{Sr}}$ phonon up in frequency. In order to get a rough idea of the magnitude of this frequency

discrepancy, we may use a simplified version of the Grüneisen approximation,^{21,22} only taking into account the contraction in the phonon polarization direction along the c axis:

$$\gamma = -(1/3)[d(\ln \nu)/d(\ln c)]. \quad (1)$$

Here γ is the mode Grüneisen parameter estimated from high-pressure Raman measurements, ν is the apical-oxygen

A_g phonon frequency, and c is the c -axis lattice parameter. In Fig. 3 (Refs. 23–35) we have plotted the observed $O(2)_{Sr}$ phonon frequencies versus La content together with the calculated frequencies derived from Eq. (1). We have used a Grüneisen parameter $\gamma \approx 0.6$ estimated from high-pressure Raman measurements of Bi2212,²⁵ since no high-pressure data on Bi2201 are available. The very similar $O(2)_{Sr}$ phonon frequencies in Bi2201 and Bi2212 justify this approximation. As a comparison we have also included data on Y123 from Refs. 32 and 33, where Sr and La have been substituted for Ba ($r_{Ba^{2+}} = 1.42 \text{ \AA}$), as well as results on Sr- and La-substituted Tl2201.^{34,35} Figure 3 shows that only in the case of Sr substitution for Ba in Y123 do the experimentally determined apical-oxygen phonon frequencies coincide with the calculated data derived from Eq. (1). The disagreement between ν_{obs} and ν_{calc} is most pronounced for Bi2201 and for the isostructural Tl2201 system. The Grüneisen approach attempted above is of course an oversimplification of the real physical problem, since the apical-oxygen A_g phonon frequencies should depend mostly on changes in the two nearest-neighbor distances in the vibration direction. In the Bi2201 case the two relevant distances would be the short $O(2)_{Sr}$ -Bi bond ($\sim 1.97 \text{ \AA}$) and the $O(2)_{Sr}$ -Cu bond ($\sim 2.58 \text{ \AA}$).^{4,5} The anomalous softening of the $O(2)_{Sr}$ mode suggests that one of these bonds expands and/or weakens upon La substitution, although the total Cu- $O(2)_{Sr}$ -Bi distance has to decrease due to the decreasing Sr/La average radius. Unfortunately, there are no published bond-distance data on La-substituted Bi2201 to verify this hypothesis. In the case of Tl2201, however, the softening of the apical-oxygen mode upon La substitution for Ba can indeed be correlated to a slight increase in the short Tl- $O(2)_{Ba}$ bond length.²⁸ We suggest that the anomalous phonon frequency dependencies observed in the La-substituted Bi2201, as well as in the La/Sr-substituted Tl2201 (Refs. 34 and 35) and La-substituted Y123,³³ are connected with “charge-redistribution” effects induced by the substitution ions. In the Bi2201 case, band-structure calculations^{36,37} indicate that the metallic state extends over the whole O_{Cu} -Cu- O_{Sr} -Bi- O_{Bi} complex. Doping electrons into this complex via La^{3+} for Sr^{2+} substitution would thus tend to increase the average electron density on both Cu and Bi, thereby decreasing the electrostatic attraction in the Cu- $O(2)_{Sr}$ -Bi bond. This should result in a softening of the $O(2)_{Sr}$ phonon. This interpretation is supported by the permanganate- and iodometric-titration experiments which indicate a valence change from $\sim Bi^{+3.09}/Cu^{+2.06}$ for $x=0$ to $\sim Bi^{+3.06}/Cu^{+1.93}$ for $x=0.8$.⁷ The same scenario should be valid when La substitutes for Ba in Y123 and Tl2201 as well, although in the Y123 case the “internal pressure” induced by the La-Ba size difference actually dominates the frequency dependence. The anomalous phonon softening reported for Sr-substituted Tl2201, has been interpreted in terms of an electron transfer from the CuO_2 plane to the Tl-O layers, resulting in a smaller electrostatic attraction between Tl and O_{Ba} .³⁴ Similar “charge-redistribution” effects accompanied by an anomalous O_{Ba} phonon softening also occur when, e.g., Co, Fe or Al is substituted for chain Cu in Y123.³² Measurements of the apical-oxygen O_{Sr}/O_{Ba} phonon, together with lattice parameter determinations, can thus be used for detection and interpretation of “charge-

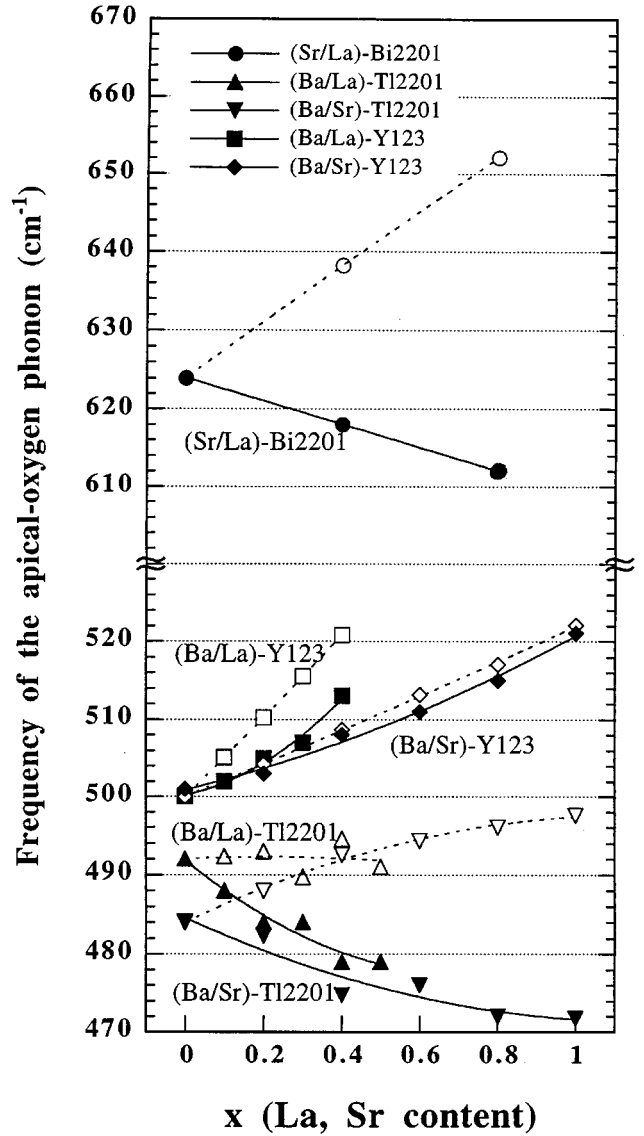


FIG. 3. Filled symbols show the observed changes in the apical-oxygen (O_{Sr} and O_{Ba}) phonon frequency upon La or Sr substitution in $Bi_2Sr_{2-x}La_xCuO_{6+d}$ (present results), $Tl_2Ba_{2-x}La_xCuO_{6+d}$ (Ref. 35), $Tl_2Ba_{2-x}Sr_xCuO_{6+d}$ (Ref. 34), $YBa_{2-x}La_xCu_3O_{6+d}$ (Ref. 33) and $YBa_{2-x}Sr_xCu_3O_{6+d}$ (Ref. 32). Open symbols show frequencies estimated from the Grüneisen approximation [Eq. (1), see text]. The calculations for Bi2201, Tl2201, and Y123 are based on Grüneisen parameters $\gamma=0.6$ (Ref. 25), $\gamma=0.5$ (Ref. 26), and $\gamma=1.35$ (Ref. 27), respectively.

redistribution” processes in a large number of high- T_c cuprates. Such information is important not only for understanding the basic physical properties of high- T_c cuprates, but also for making “educated guesses” on how to optimize the carrier concentration with respect to T_c through a chemical substitution.

IV. CONCLUSION

Polarized Raman spectra of $Bi_2Sr_{2-x}La_xCuO_{6+d}$ single crystals have been measured under the five main scattering configurations, including the c -axis polarized geometry.

From the polarization dependence and a comparison with previous reports on Bi2212 and Bi1212, we identify the $4A_{1g}$ symmetry modes that are Raman allowed within the ideal body-centered tetragonal unit cell. In contrast to most previous reports on Bi2201 we propose that the strongly *c*-axis polarized band around 624 cm^{-1} is due to the $\text{O}(2)_{\text{Sr}} A_{1g}$ phonon, while the exclusively *ab*-plane polarized band at $\sim 454\text{ cm}^{-1}$ is induced by the $\text{O}(3)_{\text{Bi}} A_{1g}$ vibration. La substitution in Bi2201 gives rise to a substantial softening of the $\text{O}(2)_{\text{Sr}}$ phonon by $\sim 12\text{ cm}^{-1}$, when *x* increases from 0 to 0.8. This is the opposite behavior to that expected from a simple Grüneisen picture, which predict a phonon hardening, i.e., an “internal-pressure” effect. The anomalous frequency dependence can be explained in terms of a “charge redistribri-

bution” induced by the La substitution, resulting in a weaker $\text{Cu-O}(2)_{\text{Sr}}\text{-Bi}$ bond.

ACKNOWLEDGMENTS

The authors would like to thank Professor H. Mazaki and S. Tochiyama, Department of Mathematics and Physics in The National Defense Academy, and Professor M. Yoshimura of the Tokyo Institute of Technology for their helpful comments. M.O. gratefully acknowledges the financial support of the Japan Society for the Promotion of Science. This work was financially supported by the Swedish Natural Science Research Council and by a Grant-in-Aid for Scientific Research (No. 08455012 and No. 4482) from the Ministry of Education, Science and Culture of Japan.

*To whom all correspondence should be addressed. Electronic address: kakihana@rlem.titech.ac.jp

¹See, for a review, C. Thomsen, in *Light Scattering in Solids VI*, edited by M. Cardona and G. Güntherodt (Springer-Verlag, Berlin, 1991).

²M. Kakihana, M. Osada, M. Käll, L. Börjesson, H. Mazaki, H. Yasuoka, M. Yashima, and M. Yoshimura, *Phys. Rev. B* **53**, 11 796 (1996).

³M. Zhiqiang, F. Chenggao, S. Lei, Y. Zhen, Y. Li, W. Yu, and Z. Yuheng, *Phys. Rev. B* **47**, 14 467 (1993).

⁴N. R. Kasanova and E. V. Antipov, *Physica C* **246**, 241 (1995).

⁵C. C. Toradi, M. A. Subramanian, J. C. Calabrese, J. Gopalakrishnan, E. M. McCarron, K. J. Morrissey, T. R. Askew, R. B. Flippen, U. Chowdhury, and A. W. Sleight, *Phys. Rev. B* **38**, 225 (1988).

⁶A. Maeda, M. Hase, T. Tsukada, K. Noda, S. Takebayashi, and K. Uchinokura, *Phys. Rev. B* **41**, 6418 (1990).

⁷Y. Idemoto, H. Tokunaga, and K. Fueki, *Physica C* **231**, 37 (1994).

⁸M. Zhiqiang, Z. Hongguang, T. Mingliang, T. Sun, X. Yang, W. Yu, Z. Jian, X. Chunyi, and Z. Yuheng, *Phys. Rev. B* **48**, 16 135 (1993).

⁹C. V. N. Rao, H. J. Trodahl, and J. L. Tallon, *Physica C* **251**, 192 (1994).

¹⁰M. Osada, M. Kakihana, S. Tochiyama, H. Yasuoka, H. Mazaki, and M. Yashima (unpublished).

¹¹T. Ishida and H. Mazaki, *Phys. Rev. B* **20**, 131 (1979).

¹²G. Burns, P. Strobel, G. V. Chandrashekar, F. H. Dakor, F. Holtzberg, and M. W. Shafer, *Phys. Rev. B* **39**, 2245 (1989).

¹³P. V. Huong, C. Lacour, and M. M’Hamdi, *J. Alloys Compd.* **195**, 691 (1993).

¹⁴R. Ilango, R. K. Rajaram, and N. Krishnamurthy, *Solid State Commun.* **74**, 797 (1990).

¹⁵J. Prade, A. D. Kulkarni, F. W. de Wette, U. Schröder, and W. Kress, *Phys. Rev. B* **39**, 2771 (1989).

¹⁶L. V. Gaspro, V. D. Kulakovskii, O. V. Mosochko, A. A. Polyanskii, and V. B. Timofeev, *Physica C* **160**, 147 (1989).

¹⁷R. Liu, M. V. Klein, P. D. Han, and D. A. Payne, *Phys. Rev. B* **45**, 7392 (1992).

¹⁸As is clearly seen in Fig. 2(c), the apical-oxygen phonon at $\sim 620\text{ cm}^{-1}$ consists of two components. For all spectra of Fig. 2(c), the two-Lorentzian fit (dashed lines) satisfactorily reproduced the spectral line shape of partly overlapping A_{1g} bands in the high-frequency region ($550\text{--}700\text{ cm}^{-1}$) within the accuracy determined by the spectral slitwidth in our experiment

($\pm 2\text{ cm}^{-1}$). With the degree of La doping we find that the line-widths (FWHM) of the 624- and 651-cm^{-1} bands decrease from $(\Gamma_{624}, \Gamma_{651}) = (36.8\text{ cm}^{-1}, 37.1\text{ cm}^{-1})$ at $x=0$ to $(25.7\text{ cm}^{-1}, 29.8\text{ cm}^{-1})$ at $x=0.8$.

¹⁹K. C. Hewitt, A. Martin, Y. H. Shi, and M. J. G. Lee, *Physica C* **216**, 463 (1993).

²⁰K. C. Hewitt, X. K. Chen, X. Meng-Burany, A. E. Curzon, and J. C. Irwin, *Physica C* **251**, 192 (1995).

²¹C. Thomsen, R. Liu, M. Bauer, A. Wittlin, L. Genzel, M. Cardona, E. Schonherr, W. Bauhofer, and W. König, *Solid State Commun.* **65**, 55 (1988).

²²H. J. Trodahl, R. G. Buckley, and C. K. Subramanian, *Phys. Rev. B* **47**, 11 354 (1993).

²³The calculations for Bi2201, Tl2201, and Y123 are based on Grüneisen parameters $\gamma=0.6$ (Ref. 25), $\gamma=0.5$ (Ref. 26), and $\gamma=1.35$ (Ref. 27), respectively.

²⁴The *c*-lattice parameters for $\text{Tl}_2\text{Ba}_{2-x}\text{La}_x\text{CuO}_{6+d}$, $\text{Tl}_2\text{Ba}_{2-x}\text{Sr}_x\text{CuO}_{6+d}$, $\text{YBa}_{2-x}\text{La}_x\text{Cu}_3\text{O}_{6+d}$, and $\text{YBa}_{2-x}\text{Sr}_x\text{Cu}_3\text{O}_{6+d}$ are chosen from Refs. 28–31, respectively.

²⁵M. Osada, M. Kakihana, H. Arashi, M. Käll, L. Börjesson, and M. Yashima (unpublished).

²⁶L. V. Gasparov, O. V. Misochko, M. I. Eremets, A. V. Lomsadze, and V. V. Struzhkin, *Sov. Phys. JETP* **71**, 945 (1991).

²⁷K. Syassen, M. Hanfland, K. Strössner, M. Holtz, W. Kress, M. Cardona, U. Schröder, J. Prade, and F. W. de Wette, *Physica C* **153-155**, 264 (1988).

²⁸C. Ström, M. Käll, J.-G. Johansson, S.-G. Eriksson, and L. Börjesson, *Physica C* **185-189**, 625 (1991).

²⁹C. Ström, M. Käll, J.-G. Johansson, S.-G. Eriksson, and L. Börjesson, *Physica C* **185-189**, 623 (1991).

³⁰P. Karen, H. Fjellgå, A. Kjekshus, and A. F. Andersen, *J. Solid State Chem.* **93**, 163 (1991).

³¹S.-G. Eriksson, J.-G. Johansson, C. Ström, L. Börjesson, M. Käll, and M. Kakihana, *Physica C* **185-189**, 893 (1991).

³²M. Kakihana, S.-G. Eriksson, L. Börjesson, J.-G. Johansson, C. Ström, and M. Käll, *Phys. Rev. B* **47**, 5359 (1993).

³³R. Wegerer, C. Thomsen, M. Cardona, H. J. Bornemann, and D. E. Morris, *Phys. Rev. B* **53**, 3561 (1996).

³⁴M. Käll, L. Börjesson, M. Kakihana, C. Ström, L.-G. Johansson, S.-G. Eriksson, and T. Larsson, *Physica C* **185-189**, 821 (1991).

³⁵D. Mihailovic, T. Mertelj, K. F. Voss, A. J. Heeger, and N. Heron, *Phys. Rev. B* **45**, 8016 (1992).

³⁶W. E. Pickett, *Rev. Mod. Phys.* **61**, 433 (1989).

³⁷P. A. Sterne and C. S. Wang, *J. Phys. C* **21**, L949 (1988).